Testing $f(R)$ gravity models with quasar x-ray and UV fluxes

Matías Leizerovich,[1,2,*] Lucila Kraiselburd,[2,3] Susana Landau,[1,4] and Claudia G. Scóccola[2,3]

[1]*Departamento de Física, Facultad de Ciencias Exactas y Naturales, Universidad de Buenos Aires, Avenida Intendente Cantilo S/N, 1428, Ciudad Autónoma de Buenos Aires, Argentina*

[2]*Consejo Nacional de Investigaciones Científicas y Técnicas (CONICET), Godoy Cruz 2290, 1425, Ciudad Autónoma de Buenos Aires, Argentina*

[3]*Facultad de Ciencias Astronómicas y Geofísicas, Universidad Nacional de La Plata, Observatorio Astronómico, Paseo del Bosque, B1900FWA La Plata, Argentina*

[4]*IFIBA—CONICET—UBA Avenida Intendente Cantilo S/N, 1428, Ciudad Autónoma de Buenos Aires, Argentina*

(Received 6 December 2021; accepted 11 April 2022; published 19 May 2022)

Recently, active galactic nuclei (AGN) have been proposed as "standardizable candles," thanks to an observed nonlinear relation between their x-ray and optical-ultraviolet (UV) luminosities, which provides an independent measurement of their distances. In this paper, we use these observables for the first time to estimate the parameters of $f(R)$ gravity models (specifically, the Hu-Sawicki and the exponential models) together with the cosmological parameters. The importance of these types of modified gravity theories lies in the fact that they can explain the late time accelerated expansion of the universe without the inclusion of a dark energy component. We have also included other observable data to the analyses such as estimates of the Hubble parameter $H(z)$ from cosmic chronometers (CCs), the Pantheon Type Ia (SnIa) supernovae compilation, and baryon acoustic oscillation (BAO) measurements. The 1σ inferred constraints using all datasets are $b \leq 0.276$, $\Omega_m = 0.304^{+0.010}_{-0.011}$, and $H_0 = 67.553^{+1.242}_{-0.936}$ for the Hu-Sawicki model, and $b = 0.785^{+0.409}_{-0.606}$ $\Omega_m = 0.305^{+0.011}_{-0.010}$ and $H_0 = 68.348^{+0.959}_{-0.760}$ for the exponential one, but we stress that for both $f(R)$ models results within 2σ are consistent with the Λ cold dark matter (CDM) model. Our results show that the allowed space parameter is restricted when both AGN and BAO data are added to CC and SnIa data, with the BAO dataset being the most restrictive one. We can conclude that both the ΛCDM model and small deviations from general relativity given by the $f(R)$ models studied in this paper are allowed by the considered observational datasets.

DOI: 10.1103/PhysRevD.105.103526

I. INTRODUCTION

The late time accelerated expansion of the Universe is still one of the most intriguing conundrums that any successful cosmological model has to explain. In 1998, two international teams (Riess *et al.* [1,2] and Perlmutter *et al.* [3]) showed independently observational evidence of this phenomena. Since then, great efforts have been made in order to explain the physical mechanism responsible for it. In the standard cosmological model [Λ cold dark matter (ΛCDM)], a cosmological constant Λ is added to the Einstein equations of general relativity,

$$R_{\mu\nu} - \frac{R}{2} g_{\mu\nu} + \Lambda g_{\mu\nu} = \kappa T_{\mu\nu}, \tag{1}$$

where $R_{\mu\nu}$ is the Riemann tensor, R is the Ricci scalar, $g_{\mu\nu}$ is the metric, $\kappa = 8\pi G$ (for $c = 1$), and $T_{\mu\nu}$ is the energy-momentum tensor. However, this proposal has several problems that have been discussed in the literature. For instance, the observational value of the cosmological constant Λ does not match the value that is expected from theoretical estimations by 60–120 orders of magnitude [4–7]. In this context, alternative cosmological models have been considered to provide an explanation for the dynamics of the Universe's expansion. These models can be classified into two families [8]: those which incorporate scalar fields with minimal coupling to gravity and matter (for example, quintessence or k-essence fields [9,10]) and those which are based in alternative gravity theories. In the last group we find theories like Gauss-Bonnet, Horndeski, and the so-called $f(R)$ theories [8,11–14], among many others. Another motivation for studying alternative cosmological models is the Hubble tension. Specifically, the value of the current Hubble parameter H_0 that has been obtained using cosmic microwave background (CMB) data and assuming a standard cosmological model [15] is not in agreement with the one using model-independent

*mleize@df.uba.ar

observations, such as the luminosity from supernovae Ia [16].[1]

$f(R)$ theories [14], despite originally being proposed by Starobinsky [19] in the 1980s to describe the inflation mechanism, have recently become relevant for explaining the late time accelerated expansion of the Universe. In these models, the Ricci scalar R on the Einstein-Hilbert action is replaced by a scalar function of R. Although many $f(R)$ were proposed in the past, the vast majority of them have been ruled out by theoretical reasons such as antigravity regimes [20] or by experimental and observational constraints such as local gravity tests [14,21,22] and solar system tests [23–27]. Two models that are still considered viable are the Hu-Sawicki [28] and the exponential ones [29–31]. Recently, Desmond and Ferreira [32], by using morphological indicators in galaxies to constrain the strength and range of the fifth force, have claimed that the Hu-Sawicki $f(R)$ model can be ruled out. In their methodology, they use general relativity (GR)-based mock catalogs to which the effects of the $f(R)$ model are added. However, the results obtained by superimposing analytical expressions for the $f(R)$ effects to a ΛCDM cosmology are different from those obtained from a modified-gravity-based simulation, such as those presented in [33].

In Nunes *et al.* [34] different $f(R)$ models (including the Hu-Sawicki and the exponential models) have been tested using cosmic chronometers (CCs), baryon acoustic oscillations (BAOs), joint light curves samples from supernovae Ia (SnIa), and astrophysical estimates of H_0. Also, Farugia *et al.* [35] have analyzed the same $f(R)$ models using several of the observational data mentioned above (but updated) plus redshift space distortions (RSD) dataset and model-dependent CMB data. In D'Agostino and Nunes [36,37], the Hu-Sawicki model has been tested with newer datasets such as gravitational waves and lensed quasars from the H0LiCOW Collaboration. In Odintsov *et al.* [30] a change of variables to express Friedmann equations for the exponential model has been proposed, while in Ref. [38] a comparison between their numerical solution and the latest updates of the aforementioned observational data has been made. In the present work, we constrain the Hu-Sawicki and the exponential models using a large set of cosmological observations, including, for the first time for these models, a recently released dataset of active galactic nuclei (AGN) compiled from Lusso *et al.* [39] and taking the astrophysical parameters β, γ, and δ from Li *et al.* [40]. This dataset together with SnIa and BAO data has recently been considered by Bargiacchi *et al.* [41] to constrain the ΛCDM model as well as extensions of the latter and to discuss implications for nonflat cosmological models.

This paper is organized as follows: In Sec. II we briefly describe the main aspects of the $f(R)$ models in the cosmological context, we recall the modified Friedmann equations, and we present the $f(R)$ models that are analyzed in this paper. In Sec. III, we describe the observational data that are used to test the predictions of the theoretical models. We also explain the statistical treatment that we have chosen for the AGN data, which is based on the one proposed in Ref. [40]. In Sec. IV, we present the results of the statistical analyses. Comparison with similar works is discussed in Sec. V, while the conclusions are presented in Sec. VI. Each $f(R)$ model considered in this paper requires a specific change of variables to solve Friedmann equation. We describe the details of this procedure the Appendix.

II. THEORETICAL MODELS

The $f(R)$ theories refer to a set of gravitational theories whose Lagrangian is given by a function of the Ricci scalar R, where each $f(R)$ defines a different model. Therefore, the Einstein-Hilbert action for these theories is

$$S = \frac{1}{2\kappa}\int d^4x\sqrt{-g}f(R) + S_m + S_r, \tag{2}$$

where S_m and S_r represent the matter and radiation actions, respectively. The field equations are obtained by varying the action S with respect to the metric $g_{\mu\nu}$ such that

$$R_{\mu\nu}f_R - \frac{1}{2}g_{\mu\nu}f(R) + (g_{\mu\nu}\Box - \nabla_\mu\nabla_\nu)f_R = \kappa T_{\mu\nu}, \tag{3}$$

where $fR = \frac{df}{dR}$, $\Box$ is the d'Alembertian operator, ∇_μ is the covariant derivative, and $T_{\mu\nu}$ is the energy-momentum tensor.

In this work we assume a spatially flat Friedmann-Lemaître-Robertson-Walker (FLRW) cosmology, so the metric is given by

$$ds^2 = -dt^2 + a^2(t)(dr^2 + r^2d\Omega^2), \tag{4}$$

where $a(t)$ is the scale factor of the Universe and $H = \dot{a}/a$ is the Hubble parameter (the dot represents the derivatives with respect to the cosmic time). Then, the Ricci scalar can be written as

$$R = 6(2H^2 + \dot{H}). \tag{5}$$

Considering the energy-momentum tensor of a perfect fluid $T^\mu_\nu = \mathrm{diag}(-\rho, P, P, P)$ (where $\rho = \rho_m + \rho_r$ and $P = P_m + P_r$), the field equations (3) become

$$-3H^2 = -\frac{1}{f_R}\left[\kappa\rho + \frac{Rf_R - f}{2} - 3H\dot{R}f_{RR}\right], \tag{6a}$$

[1]There is also no agreement within the scientific community of the amount of this tension. While some authors claim that there is a 4-σ tension [16], others claim lower amounts or even no disagreements [17,18].

$$-2\dot{H} = \frac{1}{f_R}[\kappa(\rho + P) + f_{RRR}\dot{R}^2 + (\ddot{R} - H\dot{R})f_{RR}], \quad (6b)$$

where f_{RR} and f_{RRR} are the second and third derivative with respect to R, respectively. It has been shown that the latter equations can be expressed as a set of first-order equations, which results in a more stable system from the numerical point of view [30,42]. There are numerous proposals in this regard. In this article we assume the change of variables proposed in Ref. [30] for the exponential model and the one used by de la Cruz-Dombriz *et al.* [42] for the Hu-Sawicki model. Both settings are described in the Appendix.

The continuity equations of matter and radiation for a flat FLRW metric can be expressed as

$$\dot{\rho} + 3H(\rho + P) = 0. \quad (7)$$

At redshifts between $0 \leq z \leq 10^4$, considering pressureless (nonrelativistic) matter and radiation (relativistic particles), the solution is $\rho = \rho_m^0 a^{-3} + \rho_r^0 a^{-4}$.

Viable $f(R)$ models must fulfill some theoretical constraints, such as having a positive gravitational constant, stable cosmological perturbations, and avoiding ghost states, among many others [28,34,43]. Therefore, to elude instabilities when curvature becomes too large at high densities,[2] it is necessary that

$$f_R > 0 \quad \text{and} \quad f_{RR} > 0, \quad \text{for } R \geq R_0, \quad (8)$$

where R_0 is the current value of the Ricci scalar. Moreover, as discussed previously, a successful cosmological model must provide an explanation for the late accelerated expansion of the Universe. For this, it is required that $f(R) \to R - 2\Lambda$ when $R \geq R_0$, where Λ is an effective cosmological constant. On the other hand, bounds from local tests of gravity such as solar system and equivalence principle tests require that a viable $f(R)$ model shows a "chameleon like" mechanism [44–46]. Lastly, the stability of a late time de Sitter solution must be guaranteed. Consequently,the following condition has to be fulfilled:

$$0 < \frac{Rf_{RR}}{f_R}(r) < 1 \quad \text{at } r = -\frac{Rf_R}{f} = -2. \quad (9)$$

Accounting for all these restrictions, the viable models can be expressed as follows:

$$f(R) = R - 2\Lambda y(R, b), \quad (10)$$

with $y(R, b)$ a function that quantifies the deviation from GR and b the distortion parameter that quantifies the effect of that deviation.

As a consequence of the restrictions described above, the behavior of these $f(R)$ models tends asymptotically to the one of the ΛCDM at large redshifts ($z \geq 10^4$), when the curvature R also becomes large [28,30,43,47]. However, the late time evolution of these theories differs from ΛCDM. Hence, if $\Omega_i = \kappa\rho_i^0/3{H_0}^2$ is the current critical density, where H_0 and ρ_i^0 refer to the current values of the Hubble parameter and density ρ_i, these quantities (Ω_i and H_0) defined in $f(R)$ models will be different from the same quantities defined in the ΛCDM model. Still, all these quantities are related through the physical matter density [28],

$$\Omega_m {H_0}^2 = \Omega_m^{\Lambda\text{CDM}}({H_0}^{\Lambda\text{CDM}})^2 = \frac{\kappa}{3}\rho_m^0. \quad (11)$$

Besides, for the ΛCDM model it holds that

$$\Omega_m^{\Lambda\text{CDM}} + \Omega_\Lambda^{\Lambda\text{CDM}} = 1, \quad (12)$$

where $\Omega_\Lambda^{\Lambda\text{CDM}} = \Lambda/3(H_0^{\Lambda\text{CDM}})^2$. It should be noted that the systems of differential equations that we use in this paper are written in terms of $\Omega_m^{\Lambda\text{CDM}}$ and $H_0^{\Lambda\text{CDM}}$, while the results of the statistical analyses will be reported in terms of the corresponding parameters defined in $f(R)$ models. Equations (11) and (12) will be useful to establish the initial conditions of the Friedmann equations. For this, the main assumption is that at high redshift the behavior of $H(z)$ in the ΛCDM and $f(R)$ models is the same. Since the observational data used in this work are at redshifts $z < 8$, the radiation terms can be neglected.

Next, we present the two $f(R)$ models analyzed in this paper:

(1) The exponential $f(R)$ model was proposed by Cognola *et al.* [29] and further discussed in [30,31,48], among many others. In this model, the proposed $f(R)$ function can be expressed as

$$f(R) = R - 2\Lambda(1 - e^{-\frac{R}{\Lambda b}}), \quad (13)$$

where b and Λ are the free parameters of the model.

(2) The currently known Hu and Sawicki model was developed by these authors in 2007 [28]. The proposed $f(R)$ function can be expressed as

$$f(R) = R - \frac{c_1 R_{\text{HS}}(R/R_{\text{HS}})^n}{c_2(R/R_{\text{HS}})^n + 1}, \quad (14)$$

where c_1, c_2, R_{HS}, and n represent the free parameters of the model. It is possible to rewrite the above expression as the one proposed in Eq. (10),

[2]Other requirements that are usually asked to ensure stability in scenarios with large curvatures are $\lim_{R\to 0} f(R) - R = 0$ and $\lim_{R\to\infty} f(R) - R =$ constant.

$$f(R) = R - 2\Lambda\left[1 - \frac{1}{1 + (\frac{R}{\Lambda b})^n}\right] \tag{15}$$

with $\Lambda = c_1 R_{\rm HS}/2c_2$ and $b = 2c_2^{1-1/n}/c_1$. It is easy to see that, when $b \to 0$, the model reduces to a ΛCDM cosmology; $f(R) \to R - 2\Lambda$. In this work, we will restrict ourselves to analyze only the case when $n = 1$.

Finally, as mentioned above, the system of equations that we choose to solve to obtain $H(z)$ in each model as well as the initial conditions and the details of dealing with numerical instabilities will be described later in the Appendix.

III. OBSERVATIONAL DATA

In this section, we present the datasets that we use to determine the values of the $f(R)$ parameters that best fit the different cosmological observations.

A. Cosmic chronometers

The CC is a method developed by Simon *et al.* [49] that allows one to determine the Hubble parameter $H(z)$ from the study of the differential age evolution of old elliptical passive-evolving[3] galaxies that formed at the same time but are separated by a small redshift interval. The method relies on computing the Hubble factor $H(z)$ from the following expression:

$$H(z) = \frac{-1}{1+z}\frac{dz}{dt}, \tag{16}$$

where dz/dt can be calculated from the ratio $\Delta z/\Delta t$ and Δ refers to the difference between the two galaxies whose properties have been described above.

The galaxies chosen for this method were formed early in the Universe, at high redshift ($z > 2-3$), with large mass ($\mathcal{M}_{\rm stars} > 10^{11}\ \mathcal{M}_\odot$), and their stellar production has been inactive since then. Hence, by observing the same type of galaxies at late cosmic time, stellar age evolution can be used as a clock synchronized with cosmic time evolution. On the other hand, dz is determined by spectroscopic surveys with high precision. The goodness of this method lies in the fact that the measurement of relative ages dt eliminates the systematic effects present in the determination of absolute ages. Furthermore, dt is independent of the cosmological model since it only depends on atomic physics and not on the integrated distance along the line of sight (redshift).

For this work, we use the most precise available estimates of $H(z)$, which are summarized in Table I.

[3]Passive evolving means that there is no star formation or interaction with other galaxies.

TABLE I. $H(z)$ estimates from the cosmic chronometers. Each column stands for the redshift of the measurement, the $H(z)$ mean value (and its standard deviation), and reference, respectively.

z	$H(z)$ (km s^{-1} Mpc^{-1})	Reference
0.09	69 ± 12	
0.17	83 ± 8	
0.27	77 ± 14	
0.4	95 ± 17	
0.9	117 ± 23	[49]
1.3	168 ± 17	
1.43	177 ± 18	
1.53	140 ± 14	
1.75	202 ± 40	
0.48	97 ± 62	[50]
0.88	90 ± 40	
0.1791	75 ± 4	
0.1993	75 ± 5	
0.3519	83 ± 14	
0.5929	104 ± 13	[51]
0.6797	92 ± 8	
0.7812	105 ± 12	
0.8754	125 ± 17	
1.037	154 ± 20	
0.07	69 ± 19.6	
0.12	68.6 ± 26.2	[52]
0.2	72.9 ± 29.6	
0.28	88.8 ± 36.6	
1.363	160 ± 33.6	[53]
1.965	186.5 ± 50.4	
0.3802	83 ± 13.5	
0.4004	77 ± 10.2	
0.4247	87.1 ± 11.2	[54]
0.4497	92.8 ± 12.9	
0.4783	80.9 ± 9	

B. Supernovae type Ia

Type Ia supernovae are one of the most luminous events in the Universe and are considered as standard candles due to the homogeneity of both its spectra and light curves. As we will explain below, the distance modulus μ can be determined from the SnIa data, and alternatively, it can also be described as

$$\mu = 25 + 5\log_{10}(d_L(z)), \tag{17}$$

where d_L the luminosity distance

$$d_L(z) = (1+z)\int_0^z \frac{dz'}{H(z')}. \tag{18}$$

Since the previous expression shows how this last magnitude depends on both the redshift z and the cosmological model [via $H(z)$], it is possible to compare the distance modulus predicted by the theories with the estimates from observations.

In this case, we are considering 1048 SnIa at redshifts between $0.01 < z < 2.3$ from the Pantheon compilation [55]. For this compilation, the observed distance modulus estimator is expressed as

$$\mu = m_B - M + \alpha x_1 + \beta c + \Delta_M + \Delta_B, \tag{19}$$

with m_B being an overall flux normalization, x_1 the deviation from the average light-curve shape, and c the mean SnIa B-V color index.[4] Meanwhile, M refers to the absolute B-band magnitude of a fiducial SnIa with $x_1 = 0$ and $c = 0$, and Δ_B refers to a distance correction based on predicted biases from simulations. Coefficients α and β define the relations between luminosity and stretch and between luminosity and color, respectively.

On the other hand, Δ_M represent a distance correction based on the mass of the SnIa's host galaxy. For this SnIa compilation, it is obtained from

$$\Delta_M = \gamma \times [1 + e^{(-(m-m_{\rm step})/\tau)}]^{-1}, \tag{20}$$

where $m_{\rm step}$ is a mass step for the split, γ is a relative offset in luminosity, and m is the mass of the host galaxy. Parameter τ symbolizes an exponential transition term in a Fermi function that defines the relative probability of masses to be on one side or the other of the split. Both $m_{\rm step}$ and τ are derived from different host galaxies samples (for details, see [55]). Finally, coefficients α, β, M, and γ are the so-called nuisance parameters of the SnIa.

These parameters are usually determined through a statistical analysis with supernovae data where a ΛCDM model is assumed. In particular Scolnic *et al.* obtain for the Pantheon sample [55] the following values: $\alpha = 0.0154 \pm 0.006$, $\beta = 3.02 \pm 0.06$, and $\gamma = 0.053 \pm 0.009$. To verify these values, we have assumed the Hu-Sawicki model and performed a statistical analysis with the same dataset allowing both the nuisance and the model parameters to vary.[5] Our estimated nuisance parameters are consistent with those computed by the Pantheon compilation within 1σ. This agreement has been also obtained in a similar analysis carried out assuming another alternative theory of gravity [57] and in [55] where extensions of the ΛCDM models were assumed. All those mentioned analyses confirm that the value of the nuisance parameters are independent of the cosmological model. Therefore, in all statistical analyses reported in Sec. IV we fix the nuisance parameters to the values published by the Pantheon compilation.

[4]Parameters m_B, x_1, and c are determined from a fit between a model of the spectral sequence SnIa and the photometric data (for details, see [55]).

[5]Given the strong degeneracies between the parameters when only SnIa data are used, we have considered a fixed value for H_0 (we have analyzed two cases: one with $H_0 = 67.4\ \mathrm{km\,s^{-1}\,Mpc^{-1}}$ [15] and another one with $H_0 = 73.5\ \mathrm{km\,s^{-1}\,Mpc^{-1}}$ [56]).

C. Baryon acoustic oscillations

Before the recombination epoch, photons and electrons were coupled through Thomson scattering, generating sound waves in the primordial plasma. Once the temperature of the Universe has dropped sufficiently as for neutral hydrogen to form, matter and radiation decouples, and the acoustic oscillations are frozen, leaving an imprint both in the cosmic microwave background and in the distribution of matter at large scales. The maximum distance that the acoustic wave could travel in the plasma before decoupling defines a characteristic scale, named the sound horizon at the drag epoch r_d. Hence, BAOs provide a standard ruler to measure cosmological distances. Several tracers of the underlying matter density field provide different probes to measure distances at different redshifts.

The BAO signal along the line of sight directly constrains the Hubble constant $H(z)$ at different redshifts. When measured in a redshift shell, it constrains the angular diameter distance $D_A(z)$,

$$D_A(z) = \frac{1}{(1+z)} \int_0^z \frac{dz'}{H(z')}. \tag{21}$$

To separate $D_A(z)$ and $H(z)$, BAOs should be measured in the anisotropic 2D correlation function, for which extremely large volumes are necessary. If this is not the case, a combination of both quantities can be measured as

$$D_V(z) = \left[(1+z)^2 D_A^2(z) \frac{z}{H(z)}\right]^{1/3}. \tag{22}$$

Currently, there are many precise measurements of BAOs obtained using different observational probes. In general, a fiducial cosmology is needed in order to measure the BAO scale from the clustering of galaxies or any other tracer of the matter density field. It is known that the standard BAO analysis gives model-independent results, and that it can be used to perform cosmological parameter inference to constrain exotic models. In particular, Bernal *et al.* [58] have demonstrated the robustness of the standard BAO analysis when studying models whose extensions to the ΛCDM model may introduce contributions not captured by the template used. They have found no significant bias in the BAO analysis for the exotic models they studied. The distance constraints presented in Table II include information about $r_d^{\rm fid}$, which is the sound horizon at the drag epoch computed for the fiducial cosmology.

Here we describe the observations used in this work. In Ross *et al.* [59], the main spectroscopic sample of Sloan Digital Sky Survey data release 7 (SDSS-DR7) galaxies is used to compute the large-scale correlation function at $z_{\rm eff} = 0.15$. The nonlinearities at the BAO scale are alleviated using a reconstruction method. The first year data release of the Dark Energy Survey [62] measured the angular diameter distance D_A/r_d at $z_{\rm eff} = 0.81$, from the

TABLE II. Distance constraints from BAO measurements of different observational probes. The table shows the redshift of the measurement, the mean value, and standard deviation of the observable, the observable that is measured in each case and the corresponding reference.

$z_{\rm eff}$	Value	Observable	Reference
0.15	4.473 ± 0.159	D_V/r_d	[59]
0.44	11.548 ± 0.559	D_V/r_d	
0.6	14.946 ± 0.680	D_V/r_d	[60]
0.73	16.931 ± 0.579	D_V/r_d	
1.52	26.005 ± 0.995	D_V/r_d	[61]
0.81	10.75 ± 0.43	D_A/r_d	[62]
0.38	$10.272 \pm 0.135 \pm 0.074$	D_M/r_d	
0.51	$13.378 \pm 0.156 \pm 0.095$	D_M/r_d	[63]
0.61	$15.449 \pm 0.189 \pm 0.108$	D_M/r_d	
0.698	17.65 ± 0.3	D_M/r_d	[64]
1.48	30.21 ± 0.79	D_M/r_d	[65]
2.3	37.77 ± 2.13	D_M/r_d	[66]
2.4	36.6 ± 1.2	D_M/r_d	[67]
0.698	19.77 ± 0.47	D_H/r_d	[64]
1.48	13.23 ± 0.47	D_H/r_d	[65]
2.3	9.07 ± 0.31	D_H/r_d	[66]
2.4	8.94 ± 0.22	D_H/r_d	[67]
0.38	$12044.07 \pm 251.226 \pm 133.002$	Hr_d (km/s)	
0.51	$13374.09 \pm 251.226 \pm 147.78$	Hr_d (km/s)	[63]
0.61	$14378.994 \pm 266.004 \pm 162.558$	Hr_d (km/s)	

projected two point correlation function of a sample of 1.3×10^6 galaxies with photometric redshifts, in an area of 1336 deg^2. The final galaxy clustering data release of the Baryon Oscillation Spectroscopic Survey [63] provides measurements of the comoving angular diameter distance D_M/r_d [related with the physical angular diameter distance by $D_M(z) = (1+z)D_A(z)$] and Hubble parameter Hr_d from the BAO method after applying a reconstruction method, for three partially overlapping redshift slices centered at effective redshifts 0.38, 0.51, and 0.61. Measurements of D_V/r_d at effective redshifts of 0.44, 0.6, and 0.73 are provided by the WiggleZ Dark Energy Survey [60]. With a sample of 147,000 quasars from the extended Baryon Oscillation Spectroscopic Survey (eBOSS) [61] distributed over 2044 square degrees with redshifts $0.8 < z < 2.2$, a measurement of D_V/r_d at $z_{\rm eff} = 1.52$ is provided. The BAO can be also determined from the flux-transmission correlations in Lyα forests in the spectra of 157,783 quasars in the redshift range $2.1 < z < 3.5$ from the SDSS-DR12 [66]. Measurements of D_M/r_d and the Hubble distance D_H/r_d [defined as $D_H = c/H(z)$] at $z_{\rm eff} = 2.33$ are provided. From the cross-correlation of quasars with the Lyα-forest flux transmission of the final data release of the SDSS-III [67], a measurement of D_M/r_d and D_H/r_d at $z_{\rm eff} = 2.4$ can be obtained. From the anisotropic power spectrum of the final quasar sample of the SDSS-IV eBOSS survey [65], measurements for D_M/r_d and D_H/r_d at $z_{\rm eff} = 1.48$ are obtained. The analysis in the configuration space of the anisotropic clustering of the final sample of luminous red galaxies from the SDSS-IV eBOSS survey [64] gives constraints on D_M/r_d and D_H/r_d at $z_{\rm eff} = 0.698$.

D. Quasar x-ray and UV fluxes

Quasars are among the most luminous sources in the Universe. Besides, they are observable at very high redshift and therefore they are regarded as promising cosmological probes. In the last years, the observed relation between the ultraviolet and x-ray emission in quasars has been used to develop a new method to convert quasars into standardizable candles [39,68,69]. In this work, we will use the recent compilation provided by Risaliti and co-workers [39] of x-ray and UV flux measurements of 2421 quasars quasi-stellar object (QSOs/AGN) which span the redshift range $0.009 \leq z \leq 7.5413$ to test the cosmological models based in alternative theories of gravity described in Sec. II. The relation between the quasar UV and x-ray luminosities can be described by the following equation:

$$\log L_{\rm X} = \gamma \log L_{\rm UV} + \beta_1, \tag{23}$$

where $L_{\rm X}$ and $L_{\rm UV}$ refer to the rest-frame monochromatic luminosities at 2 keV and 2500 Å, respectively. The constants γ and β_1 are determined with observational data and should be independent of redshift in order to assure the robustness of the method [39,68,69]. It was pointed out in [39] that there is a strong correlation between the parameters involved in the quasar luminosity relation and cosmological distances; therefore, in order to test cosmological models, luminosity distances obtained from quasar fluxes should be cross-calibrated previously using, for example, data from type Ia supernovae. In this work, we use the calibration method proposed by Li *et al.* [40] which uses a Gaussian process regression to reconstruct the expansion history of the Universe from the latest type Ia supernova observations.[6] Next, we will briefly describe how this method, which is almost model independent, is implemented. Equation (23) can be expressed in terms of the UV and x-ray fluxes as follows:

$$\log F_{\rm X} = \gamma \log F_{\rm UV} + 2(\gamma - 1)\log(d_L H_0) + \beta, \tag{24}$$

where d_L refers to the luminosity distance and $\beta = \beta_1 + (\gamma - 1)\log 4\pi - 2(\gamma - 1)\log H_0$.[7] From Eq. (24), the quantity $\log F_X^{\rm SN}$ can be defined and computed, using quasar measurements of $F_{\rm UV}$, while the quantity $d_L H_0$ is obtained from

[6]Within the Gaussian process, a theoretical model is assumed but it has been discussed in [40] that the results are independent from this choice.

[7]It should be stressed that the parameter β defined here is different from the one defined in Refs. [39,69].

a Gaussian process regression method with the latest SnIa data [40]. Furthermore, the following likelihood is assumed:

$$\ln\mathcal{L} = -\frac{1}{2}\sum_i\left(\frac{\log\left(F_X(\gamma,\beta)\right)_i^{\mathrm{SN}} - \log\left(F_X\right)_i^{\mathrm{QSO}}}{s_i^2}\right) + \ln s_i^2, \tag{25}$$

where $s_i^2 = \sigma^2_{\log F_X} + \gamma^2\sigma^2_{\log F_{\mathrm{UV}}} + \delta^2$ and δ is an intrinsic dispersion that is introduced to alleviate the Eddington bias [39,69]. In such way, considering the x-ray fluxes from quasar data ($\log F_X^{\mathrm{QSO}}$), Li *et al.* [40] obtained γ, β, and δ in a model-independent way. Their results are consistent within 1σ with the ones obtained in [39] using Eq. (24). Moreover, the independence of the $L_{\mathrm{X}} - L_{\mathrm{UV}}$ relation with redshift has been analyzed in previous works [39,68,69]. In such way, we will test the cosmological models defined in Sec. II, using the following likelihood and assuming the values of γ and β obtained in [40] ($\gamma = 0.648 \pm 0.007$, $\beta = 7.730 \pm 0.244$)[8]:

$$\ln\mathcal{L} = -\frac{1}{2}\sum_i\frac{[\log(d_L H_0(\theta))_i^{\mathrm{TH}} - \log(d_l H_0)_i^{\mathrm{QSO}}]^2}{\sigma^2_{\log(d_L H_0)}}, \tag{26}$$

where $\theta = (\Omega_m^{\Lambda\mathrm{CDM}}, H_0^{\Lambda\mathrm{CDM}}, b)$, $\log(d_L H_0(\theta))^{\mathrm{TH}}$ refers to the theoretical prediction of the luminosity distance, $\log(d_L H_0)_i^{\mathrm{QSO}}$ is calculated from Eq. (24), and

$$\sigma^2_{\log(d_L H_0)} = \frac{\sigma^2_{F_{\mathrm{X}}} + \gamma^2\sigma^2_{F_{\mathrm{UV}}} + \sigma^2_\beta}{[2(\gamma-1)]^2} + \frac{(\beta + \log F_{\mathrm{UV}} - \log F_X)^2\sigma^2_\gamma}{[2(\gamma-1)^2]^2}. \tag{27}$$

On the other hand, it has been argued recently that some of the subsamples of the dataset provided in [39] are not standardizable and have model and/or redshift dependence [71–73]. First of all, the analysis used to reach such a conclusion does not include any previous cross-calibration with supernovae data. It should also be noted that the most important differences in the values of γ and β obtained in these works are for models with different geometries, i.e, flat and nonflat models. Moreover, the present work is restricted to flat $f(R)$ models. Furthermore, these analyses intend to constrain Ω_m and H_0 at the same time and it is well known that this cannot be done when using only data with information about the luminosity distances.

[8]It should be noted that the considered value of γ is in agreement with the one obtained in Ref. [41,70], where also the AGN, SnIa, and BAO datasets are used and extensions of the ΛCDM cosmological models are considered. However, in the statistical analyses of Ref. [41] γ is free to vary together with the cosmological parameters. Regarding the parameter β, there is not a fair comparison to be made since the parameter β in Ref. [41] refers to the parameter β_1 in Eq. (23) and it is necessary to fix the value of H_0 to relate both parameters.

IV. RESULTS

In this section we present the results of our statistical analysis for both models: Hu-Sawicki with $n = 1$ (HS) and the exponential $f(R)$ (EM). As we have described in Sec. II, the free parameters of these models are the distortion parameter b, the mass density Ω_m, and the Hubble parameter H_0. To do the statistical analysis, we use a Markov chain Monte Carlo method and the observational data described in Sec. III. In cases where the SnIa observational data are used, M_{abs} is also set as a free parameter. The priors used in this work are $H_0 \in [60, 80]$, $\Omega_m \in [0.01, 0.4]$, $M_{abs} \in [-22, -18]$, and $b \in [0, 5]$ for EM, while for HS $b \in [0, 2]$. To perform the numerical integration and the statistical analyses, we developed our own PYTHON code which uses SCIPY [74] and EMCEE [75] PYTHON libraries and is publicly available in a GitHub repository[76].

Table III and Fig. 1 show the results for the two $f(R)$ models detailed in Sec. II and the datasets described in Sec. III. Furthermore, we include the results for the ΛCDM model for comparison.

A. The Hu-Sawicki model

We emphasise that when the AGN or BAO data are added to the CC + SnIa analysis, the allowed parameter space is considerably reduced. We note that the BAO dataset is much more restrictive than AGN. Nevertheless, the constraining power of AGN is clearly seen. Besides, the AGN data shift the fitted value of Ω_m to larger values (this fact has been already mentioned in [40] for the ΛCDM model) and the estimated H_0 to lower values. We also notice that the shift on Ω_m (to larger values) and H_0 (to lower values) is much more pronounced for AGN than for BAO.

Regarding the relation between b and H_0, we mention that BAO data constrain the parameter space in such a way that there is a negative correlation between them. Besides, it follows from Fig. 1 that Ω_m and b show degeneracies when CC and SnIa are considered and also where the AGN data are added to the latter. We also remark that BAO reduces the allowed region of Ω_m considerably. Moreover, we note that the correlation between Ω_m and H_0 changes sign when BAO data are used, independent of whether the AGN data are used or not.

Lastly, for all datasets detailed in Table III, the b values presented are consistent with zero (ΛCDM prediction) within 1σ, except for the case where CC, SnIa, and BAO data were used together, in which the concordance is given at 2σ. The rest of the estimated free parameters are in agreement with those obtained for the ΛCDM model.

B. The exponential model

We note that the behavior of this model is very similar to the Hu-Sawicki one regarding the constraining power of the

TABLE III. Results from statistical analysis using data from CCs, luminosity distances reported by Pantheon Collaboration (SnIa), AGN UV and x-ray luminosities, and several datasets from cosmological distances of BAOs. For each parameter, we present the mean value and the 68% (95%) confidence levels or the upper limits obtained.

		M_{abs}	Ω_m	b	H_0
ΛCDM	CC + SnIa	$-19.379^{+0.056(0.109)}_{-0.053(0.104)}$	$0.301^{+0.019(0.041)}_{-0.022(0.038)}$	...	$69.034^{+1.687(3.629)}_{-2.000(3.648)}$
	CC + SnIa + AGN	$-19.407^{+0.058(0.103)}_{-0.049(0.107)}$	$0.327^{+0.016(0.034)}_{-0.019(0.036)}$	...	$67.813^{+1.728(3.399)}_{-1.775(3.465)}$
	CC + SnIa + BAO	$-19.395^{+0.024(0.051)}_{-0.025(0.049)}$	$0.297^{+0.010(0.021)}_{-0.011(0.021)}$	...	$68.564^{+0.689(1.411)}_{-0.722(1.428)}$
	CC + SnIa + BAO + AGN	$-19.384^{+0.025(0.048)}_{-0.025(0.051)}$	$0.306^{+0.010(0.020)}_{-0.011(0.019)}$	...	$68.786^{+0.729(1.469)}_{-0.729(1.404)}$
HS	CC + SnIa	$-19.374^{+0.054(0.103)}_{-0.051(0.105)}$	$0.269^{+0.036(0.059)}_{-0.028(0.062)}$	$\leq 0.623(1.348)$	$69.004^{+1.746(3.482)}_{-1.837(3.602)}$
	CC + SnIa + AGN	$-19.409^{+0.052(0.105)}_{-0.052(0.100)}$	$0.322^{+0.018(0.037)}_{-0.018(0.035)}$	$\leq 0.150(0.398)$	$67.622^{+1.656(3.344)}_{-1.751(3.403)}$
	CC + SnIa + BAO	$-19.436^{+0.037(0.066)}_{-0.032(0.071)}$	$0.292^{+0.012(0.022)}_{-0.011(0.022)}$	$0.294^{+0.084(0.400)}_{-0.269(0.294)}$	$66.950^{+1.389(2.247)}_{-1.041(2.436)}$
	CC + SnIa + BAO + AGN	$-19.414^{+0.034(0.060)}_{-0.029(0.064)}$	$0.304^{+0.010(0.020)}_{-0.011(0.021)}$	$\leq 0.276(0.583)$	$67.553^{+1.242(2.029)}_{-0.936(2.255)}$
EM	CC + SnIa	$-19.376^{+0.055(0.108)}_{-0.054(0.109)}$	$0.293^{+0.025(0.049)}_{-0.022(0.051)}$	$\leq 1.102(2.015)$	$68.998^{+1.880(3.705)}_{-1.850(3.621)}$
	CC + SnIa + AGN	$-19.403^{+0.055(0.104)}_{-0.052(0.105)}$	$0.324^{+0.019(0.038)}_{-0.019(0.037)}$	$\leq 0.749(1.272)$	$67.903^{+1.699(3.410)}_{-1.789(3.434)}$
	CC + SnIa + BAO	$-19.405^{+0.031(0.055)}_{-0.025(0.056)}$	$0.298^{+0.011(0.022)}_{-0.011(0.021)}$	$\leq 1.155(1.928)$	$68.011^{+1.136(1.833)}_{-0.777(2.079)}$
	CC + SnIa + BAO + AGN	$-19.393^{+0.028(0.053)}_{-0.026(0.055)}$	$0.305^{+0.011(0.020)}_{-0.010(0.021)}$	$0.785^{+0.409(0.760)}_{-0.606(0.785)}$	$68.348^{+0.959(1.704)}_{-0.760(1.771)}$

BAO and AGN datasets. In fact, the constraints on Ω_m, b, and H_0 are considerably reduced when either dataset is included in the analysis, BAO being the most restrictive one. Also, we note that the values of Ω_m and H_0 are also shifted when the AGN dataset is added in the same way described previously for the HS model.

As regards the correlation between parameters, there is no clear relation between b and H_0 and the same is observed for the case of b and Ω_m. Conversely, the inclusion of BAO data makes the correlation between Ω_m and H_0 to change sign, the same effect we have already discussed for the HS model.

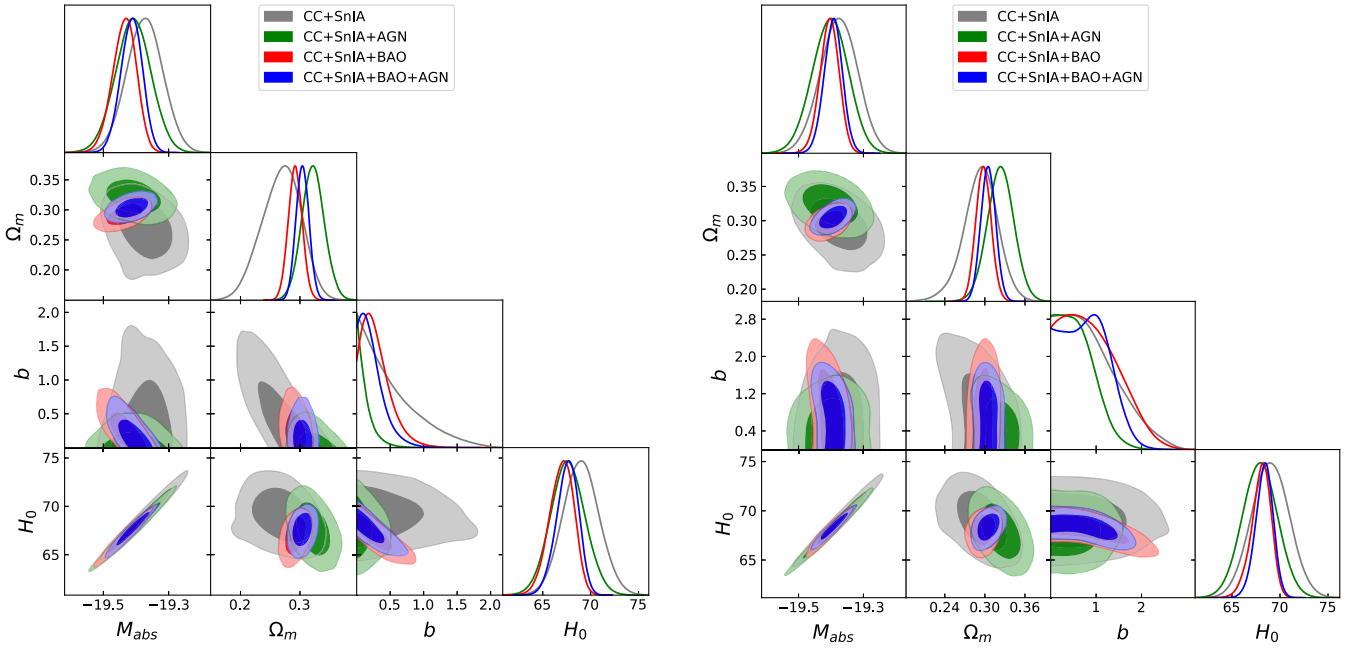

FIG. 1. Results of the statistical analysis for the $f(R)$ Hu-Sawicki model (left) and the exponential model (right). The darker and brighter regions correspond to 65% and 95% confidence regions, respectively. The plots in the diagonal show the posterior probability density for each of the free parameters of the model.

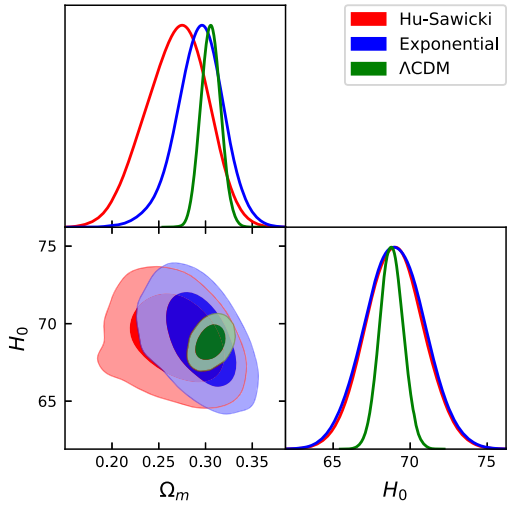

FIG. 2. Results for the matter density Ω_m and the Hubble parameter H_0 using all the datasets (CC + SnIa + BAO+ AGN). The plots show the 68% and 95% confidence region together with the posterior probability density for each parameter obtained for the two $f(R)$ models considered in this paper and the ΛCDM model.

On the other hand, we point out that the obtained intervals for the distortion parameter b are larger than the ones of the Hu-Sawicki model. This is expected since it is necessary a bigger change on b (in EM) to notice a difference with the ΛCDM model predictions. Furthermore, the constraints on H_0 and Ω_m are in agreement with those obtained for ΛCDM model for all statistical analyses carried out in this paper. Besides, the estimated b constraints are consistent at 1σ with the ΛCDM model ($b = 0$), except for the case where the CC + SnIa + BAO + AGN data were used; for the latter the consistency is within 2σ.

Figure 2 shows that the allowed parameter space for Ω_m and H_0 is enlarged with respect of the ΛCDM case and also the sign of the correlation changes when either the HS or the exponential model are considered. Finally, we also note that the parameter spaces obtained for the Hu-Sawicki and the exponential $f(R)$ models are compatible at 1σ in all the studied cases.

V. DISCUSSION

Here we compare our results shown in the previous section with others that have already been published by other authors for the same $f(R)$ models using the same and/or similar datasets ([35,37] for HS and [35,38] for EM). We show in Fig. 3 a comparison of our results with the ones obtained by other authors for the Hu-Sawicki model and the same is done in Fig. 4 for the exponential model.

Our parameter estimates for the Hu-Sawicki model using CC + SnIa data are 1σ consistent with the ones published in [37] for the same data compilations. The b values reported in there are slightly smaller at 1σ and smaller at 2σ than ours. These differences are due to the fact that, in that work, the authors only use the series expansion proposed by Basilakos *et al.* [78] to obtain an expression for $H(z)$ [79], while we use the combination of methods explained in Sec. B of the Appendix. That series expansion only allows them to explore a small range of b values ($b < 1$) which does not deviate much from the ΛCDM prediction; this does not happen in our analysis, where the parameter space to be examined is much larger. Furthermore, in that article another statistical analysis is performed incorporating data from six systems of strongly lensed quasars analyzed by the H0LiCOW Collaboration [77] to the data mentioned before (CC + SnIa). Comparing the results of this analysis with our own, it is noticed that (i) the ranges of H_0 are in agreement within 2σ except for our study of CC + SnIa + BAO and CC + SnIa + BAO + AGN; (ii) the Ω_m intervals are consistent at 1σ except for our CC + SnIa + AGN analysis, where they are consistent at 2σ; and (iii) all the b ranges are compatible at 1σ. Another interesting result to compare with is the one published by Farugia *et al.* [35]. Although their results are in agreement with ours with 1σ, their estimated range of b values is very small (of the order 10^{-4}). They use the same data compilations as we do for CC and SnIa but our BAO dataset is different, plus they add data from RSD and

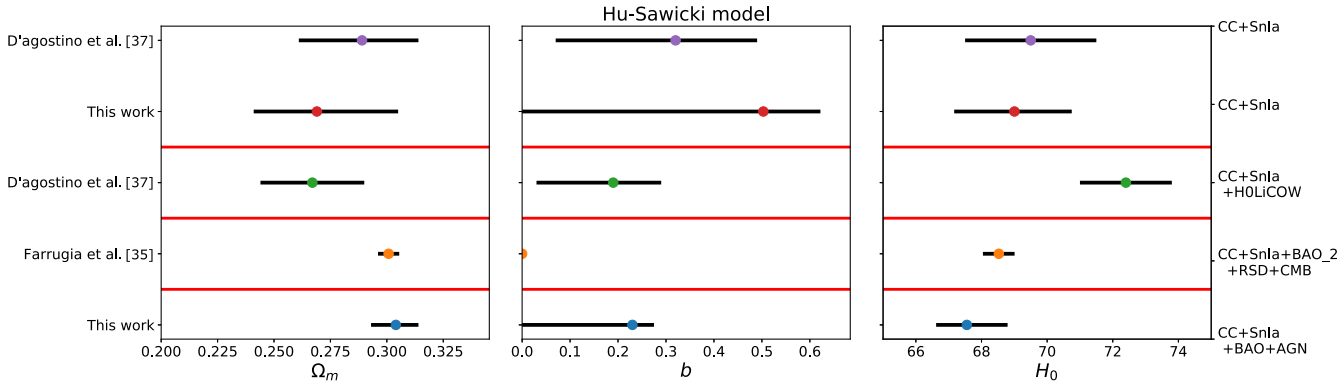

FIG. 3. Constraints on the free parameters of the Hu-Sawicki model. Comparison between the 1σ confidence intervals obtained in this work and the ones reported by other authors.

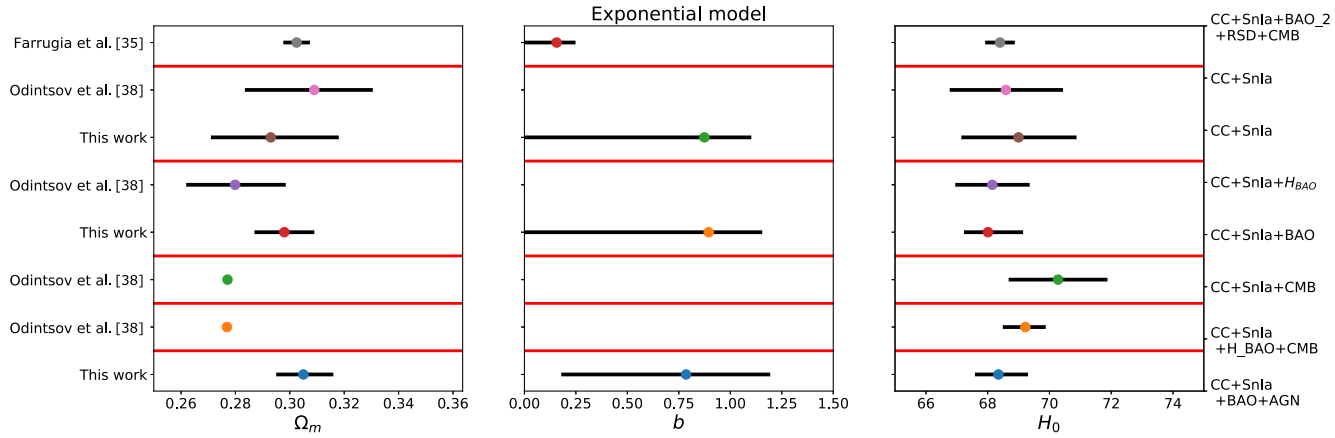

FIG. 4. Constraints on the free parameters of the exponential model. Comparison between the 1σ confidence intervals obtained in this work and the ones reported by other authors.

CMB. It should be noted that the CMB data used in [35] refer to the acoustic scale l_A, the shift parameter R, and the current baryon density $\omega_b = \Omega_b h^2$. However, these observables are obtained through a statistical analysis where a ΛCDM model is assumed. Therefore, in our opinion, it is not correct to use these data to constrain alternative cosmological models.

On the other hand, the estimates we have obtained for the parameters of the exponential $f(R)$ model using CC and SnIa data are consistent at 1σ with the values of Ω_m and H_0 reported in [38] for the same dataset. However, in that paper, the b interval is not reported, but it is for an associate quantity $\beta = 2/b$. In order to compare it with our predictions, we tried to construct the posterior distribution for β based on our distribution for b. Since the results are located near $b = 0$, the distribution for β tends to infinity on the ranges of interest (as it is noticed in that article), so it cannot be sampled correctly. These authors also perform statistical tests using data from H_{BAO} (a BAO dataset different than ours) and CMB, which both further restrict the parameter space. Their estimates using $\mathrm{CC} + \mathrm{SnIa} + H_{\mathrm{BAO}}$ are compatible with ours (for $\mathrm{CC} + \mathrm{SnIa} + \mathrm{BAO}$ dataset) at 1σ, while their predictions using $\mathrm{CC} + \mathrm{SnIa} + H_{\mathrm{BAO}} + \mathrm{CMB}$ are consistent with ours (using $\mathrm{CC} + \mathrm{SnIa} + \mathrm{BAO} + \mathrm{AGN}$) within 1σ only for the H_0 intervals, since the CMB data greatly reduce the Ω_m interval. Finally, in article [35] a statistical analysis is also performed for the exponential model using the $\mathrm{CC} + \mathrm{SnIa} + \mathrm{BAO}_2 + \mathrm{RSD} + \mathrm{CMB}$ data (BAO_2 is a BAO dataset different than ours), whose results are consistent within 1σ with ours (using $\mathrm{CC} + \mathrm{SnIa} + \mathrm{BAO} + \mathrm{AGN}$) but their parameter intervals are narrower than ours. It should not be overlooked that the CMB data used in both papers [35,38] are biased as explained above. Finally, from all the statistical analyses that have been performed in this paper, it is noted that, for the models studied here, the estimated H_0 parameters are consistent with the latest result reported by the Planck Collaboration [15] within 1σ but not with the ones published by Riess *et al.* ([16,56]). Besides, the obtained Ω_m confidence intervals are consistent with the ones obtained by the Planck Collaboration [15] within 1σ except for our $\mathrm{CC} + \mathrm{SnIa}$ and $\mathrm{CC} + \mathrm{SnIa} + \mathrm{BAO} + \mathrm{AGN}$ analyses with the Hu-Sawicki model, where the agreement is within 2σ.

VI. CONCLUSIONS

In this article we have analyzed two $f(R)$ models (HS and EM) in a cosmological context. For this, we have solved the corresponding Friedmann equations and we have performed statistical analyses considering recent datasets from SnIa, BAO, AGN, and CC in order to constrain the free parameters of the models. The originality of this work lies in the use of AGN (not previously used for these particular theories) as standard candles to put bounds to the proposed models and the inclusion of the latest BAO data from the eBOSS Collaboration (2020). Furthermore, we have previously verified the consistency between the SnIa nuisance parameters published by the Pantheon Collaboration assuming a ΛCDM cosmological model and those estimated from the $f(R)$ models studied here.

Our results show that, although AGN narrow down the parameter space of cosmological models more than the SnIa and CC data, the baryon acoustic oscillation data continue to be the most restrictive ones. On the other hand, all our estimates for the different combinations of datasets are in accordance within 2σ with the values reported by other authors for the same cosmological models but with different datasets. Moreover, we have found that the H_0 estimates are consistent with the value reported by the Planck Collaboration. The 1σ obtained constraints when using the $\mathrm{CC} + \mathrm{SnIa} + \mathrm{BAO} + \mathrm{AGN}$ dataset for the Hu-Sawicki model are $b \leq 0.276$, $\Omega_m = 0.304^{+0.010}_{-0.011}$, and $H_0 = 67.553^{+1.242}_{-0.936}$, and for the exponential model, $b = 0.785^{+0.409}_{-0.606}$, $\Omega_m = 0.305^{+0.011}_{-0.010}$, and $H_0 = 68.348^{+0.959}_{-0.760}$. We stress that results within 2σ are in agreement with the ΛCDM model.

In summary, we have analyzed the Hu-Sawicki and the exponential $f(R)$ predictions with different and new datasets. Moreover, although the b estimates are in agreement with the ΛCDM prediction at 2σ, the allowed region of the parameter space leads us to conclude that both HS and exponential $f(R)$ models are not yet ruled out by current data to explain the late time accelerated expansion of the Universe.

ACKNOWLEDGMENTS

The authors would like to thank G. S. Sharov, R. Nunes, G. Bargiacchi, X. Li, S. Kandhai, H. Desmond, M. Salgado, B. Li, S. Pérez Bergliaffa, E. Colgáin, and L. Perivolaropoulos for their helpful comments. The authors are supported by the National Agency for the Promotion of Science and Technology (ANPCYT) of Argentina Grant No. PICT-2016-0081, CONICET Grant No. PIP 11220200100729CO, and Grants No. G140, No. G157, No. G175 from UNLP and Grant No. 20020170100129BA UBACYT.

APPENDIX: SOLVING THE FRIEDMANN EQUATIONS

In general, the Friedmann equations (6) are not easy to solve. In fact, it is a usual procedure to resolve them numerically. For this reason, it is desirable to improve the system stability and to speed up the computation time by choosing an appropriate parametrization for each model. In the following, we provide details of the numerical integration in each case including the initial conditions and the way of dealing with numerical instabilities.

1. The exponential model

For the exponential model, it is very useful to express the Friedmann equations in terms of a new set of variables as follows [30]:

$$\frac{dH}{dx} = \frac{R}{6H} - 2H, \tag{A1a}$$

$$\frac{dR}{dx} = \frac{1}{f_{RR}}\left(\frac{\kappa\rho}{3H^2} - f_R + \frac{Rf_R - f}{6H^2}\right), \tag{A1b}$$

$$\frac{d\rho}{dx} = -3(\rho + P). \tag{A1c}$$

Here $x = \log a = -\log(z+1)$ is the number of e-folds, with $a(t_0) = 1$ at the present time t_0. Using the following dimensionless change of variables,

$$E = \frac{H}{H_0{}^{\Lambda\mathrm{CDM}}}, \qquad \mathcal{R} = \frac{R}{2\Lambda}, \tag{A2}$$

the field equations are expressed in terms of the parameters $\Omega_m^{\Lambda\mathrm{CDM}}$, $\Omega_\Lambda^{\Lambda\mathrm{CDM}}$, and $H_0{}^{\Lambda\mathrm{CDM}}$ as

$$\frac{dE}{dx} = \Omega_\Lambda^{\Lambda\mathrm{CDM}}\frac{\mathcal{R}}{E} - 2E, \tag{A3a}$$

$$\frac{d\mathcal{R}}{dx} = \frac{2\Lambda}{f_{\mathcal{R}\mathcal{R}}}\left[\Omega_m^{\Lambda\mathrm{CDM}}\frac{a^{-3} + X^{\Lambda\mathrm{CDM}}a^{-4}}{E^2} - \frac{f_\mathcal{R}}{2\Lambda} + \frac{\mathcal{R}f_\mathcal{R} - f}{6(H_0^{\Lambda\mathrm{CDM}})^2E^2}\right], \tag{A3b}$$

where $X^{\Lambda\mathrm{CDM}} = \Omega_r^{\Lambda\mathrm{CDM}}/\Omega_m^{\Lambda\mathrm{CDM}}$, and $f_\mathcal{R}$ and $f_{\mathcal{R}\mathcal{R}}$ are the first and second derivative with respect to $\mathcal{R}$. This system of equations is solved numerically by establishing appropriate initial conditions.

It has been already discussed that there are two situations in which the behavior of the model tends asymptotically to the ΛCDM solution: (i) high redshifts (large curvature) and (ii) $b \to 0$. Therefore, to perform the numerical integration we can assume initial conditions that match the ΛCDM model at a redshift z_i [$x_i = -\log(z_i + 1)$], i.e.,

$$E^2(x_i) = \Omega_m^{\Lambda\mathrm{CDM}}(e^{-3x_i} + X^{\Lambda\mathrm{CDM}}e^{-4x_i}) + \Omega_\Lambda^{\Lambda\mathrm{CDM}}, \tag{A4a}$$

$$\mathcal{R}(x_i) = 2 + \frac{\Omega_m^{\Lambda\mathrm{CDM}}}{2\Omega_\Lambda^{\Lambda\mathrm{CDM}}}e^{-3x_i}. \tag{A4b}$$

In order to determine z_i, we assume that $f(R(z_i)) \simeq R - 2\Lambda$. This condition can be expressed as follows [30]:

$$e^{-\frac{R(z_i)}{\Lambda b}} \simeq \epsilon = 10^{-10}. \tag{A5}$$

In turn, this implies

$$z_i = \left[\frac{\Omega_\Lambda b}{\Omega_m}\left(\ln\epsilon^{-1} - \frac{4}{b}\right)\right]^{1/3} - 1. \tag{A6}$$

Thus, when $z > z_i$ we consider the solution of the exponential model as the ΛCDM one and when $z < z_i$ the prediction of the model is calculated from the numerical integration of Eqs. (A3a) and (A3b).

2. Hu-Sawicki model

For this model, the numerical integration of $H(z)$ performed with the change of variables proposed in [30] is much more computationally expensive than the one accomplished with the proposal of de la Cruz-Dombriz *et al.* [42].[9] Consequently, we implement the latter such that

$$x = \frac{\dot{R}f_{RR}}{Hf_R}, \tag{A7a}$$

[9]Besides, the system of equations proposed in [42] is also not the most appropriate for the exponential model.

$$y = \frac{f}{6H^2 f_R}, \tag{A7b}$$

$$v = \frac{R}{6H^2}, \tag{A7c}$$

$$\Omega = \frac{8\pi G\rho_m}{3H^2 f_R}, \tag{A7d}$$

$$\Gamma = \frac{f_R}{R f_{RR}}, \tag{A7e}$$

$$r = R/R^*, \tag{A7f}$$

where the constant R^* has the same units as the Ricci scalar R (in this case, $R^* = R_{\rm HS}$). From this change of variables, the FLRW equations (6) and (7) become

$$\frac{dH}{dz} = \frac{H}{z+1}(2 - v), \tag{A8a}$$

$$\frac{dx}{dz} = \frac{1}{z+1}(-\Omega - 2v + x + 4y + xv + x^2), \tag{A8b}$$

$$\frac{dy}{dz} = \frac{-1}{z+1}(vx\Gamma - xy + 4y - 2yv), \tag{A8c}$$

$$\frac{dv}{dz} = \frac{-v}{z+1}(x\Gamma + 4 - 2v), \tag{A8d}$$

$$\frac{d\Omega}{dz} = \frac{\Omega}{z+1}(-1 + 2v + x), \tag{A8e}$$

$$\frac{dr}{dz} = -\frac{x\Gamma r}{z+1}. \tag{A8f}$$

The latter system of equations is also solved numerically by defining the proper initial conditions.

When b tends to zero, the numerical integration of Eqs. (A8) is particularly computationally expensive, becoming unstable for certain combinations of the parameters b and Ω_m^0. This occurs because, when the models $f(R)$ resemble ΛCDM, f_{RR} tends to zero. To avoid this problem, Basilakos *et al.* [78] proposed a method to obtain a series expansion of H(z) around $b = 0$ (the ΛCDM model solution). In this way, there is no need to perform the numerical integration in those regions of the parameter space that require large computational times. This approach was also used in many works such as [34,36,37]. The general idea of this procedure is as follows: letting $N = -\log(1+z)$ be the number of e-foldings at redshift z, then the Hubble parameter of the ΛCDM model can be written as

$$H^2_{\Lambda\rm CDM}(N) = (H_0^{\Lambda\rm CDM})^2[\Omega_m^{\Lambda\rm CDM} e^{-3N} + (1 - \Omega_m^{\Lambda\rm CDM})], \tag{A9}$$

and an expansion around it will be given by

$$H^2(N) = H^2_{\Lambda\rm CDM}(N) + \sum_{i=1}^{M} b^i \delta H_i^2(N), \tag{A10}$$

where M is the number of terms that are used for the expansion. It has been studied that, for the Hu-Sawicki model with $n = 1$, the error in assuming expression (A10) just keeping the first two nonzero terms of the expansion (instead of the numerical integration) is of order of 0.001% for all redshifts and $b \leq 0.5$ (for details, see [78]). Unfortunately, this method cannot be applied to the exponential $f(R)$ model since it cannot be expanded in series around $b = 0$.

In a nutshell, for $b \leq 0.15$, we use Eq. (A10) up to order 2 in b, while for other values of b we solve Eqs. (A8) numerically. For this last case, as we did for the exponential model, the initial conditions of the system of Eqs. (A8) are established so that the behavior of the $f(R)$ model matches the one of the ΛCDM model,

$$x_i = 0, \tag{A11a}$$

$$y_i = \frac{(R_i - 2\Lambda)}{6H_i^2}, \tag{A11b}$$

$$v_i = \frac{R_i}{6H_i^2}, \tag{A11c}$$

$$\Omega_i = 1 - v_i + x_i + y_i, \tag{A11d}$$

$$r_i = R_i/R_{\rm HS}, \tag{A11e}$$

where $R_i = R^{\Lambda\rm CDM}(z_i)$ and $H_i = H^{\Lambda\rm CDM}(z_i)$ are the values of the Ricci tensor and the Hubble parameter on the initial condition, respectively. In this paper, the initial redshift for the Hu-Sawicki model is set at $z_i = 10$. For both models, we have checked that the obtained solutions of the Friedmann equations do not depend on the particular choice of the initial redshift provided z_i is sufficiently large ($z_i \geq 5$).[10]

[10]In fact, the percentage difference between solutions where $5 \leq z_i < 10$ and the one assumed in this paper is less than 0.3%.

[1] A. G. Riess, A. V. Filippenko, P. Challis, A. Clocchiatti, A. Diercks, P. M. Garnavich, R. L. Gilliland, C. J. Hogan, S. Jha, R. P. Kirshner *et al.*, Astron. J. **116**, 1009 (1998).

[2] B. P. Schmidt, N. B. Suntzeff, M. M. Phillips, R. A. Schommer, A. Clocchiatti, R. P. Kirshner, P. Garnavich, P. Challis, B. Leibundgut, J. Spyromilio *et al.*, Astrophys. J. **507**, 46 (1998).

[3] S. Perlmutter, G. Aldering, G. Goldhaber, R. A. Knop, P. Nugent, P. G. Castro, S. Deustua, S. Fabbro, A. Goobar, D. E. Groom *et al.*, Astrophys. J. **517**, 565 (1999).

[4] S. Weinberg, Rev. Mod. Phys. **61**, 1 (1989).

[5] R. Bousso, Gen. Relativ. Gravit. **40**, 607 (2008).

[6] S. M. Carroll, Living Rev. Relativity **4** (2001).

[7] V. Sahni and A. Starobinsky, Int. J. Mod. Phys. D **09**, 373 (2000).

[8] T. Clifton, P. G. Ferreira, A. Padilla, and C. Skordis, Phys. Rep. **513**, 1 (2012).

[9] A. Joyce, L. Lombriser, and F. Schmidt, Annu. Rev. Nucl. Part. Sci. **66**, 95 (2016).

[10] S. Tsujikawa, Classical Quantum Gravity **30**, 214003 (2013).

[11] B. Li, J. D. Barrow, and D. F. Mota, Phys. Rev. D **76**, 044027 (2007).

[12] G. W. Horndeski, Int. J. Theor. Phys. **10**, 363 (1974).

[13] T. Kobayashi, M. Yamaguchi, and J. Yokoyama, Prog. Theor. Phys. **126**, 511 (2011).

[14] A. D. Felice and S. Tsujikawa, Living Rev. Relativity **13**, 3 (2010).

[15] N. Aghanim, Y. Akrami, M. Ashdown, J. Aumont, C. Baccigalupi, M. Ballardini, A. J. Banday, R. B. Barreiro, N. Bartolo *et al.* (Planck Collaboration), Astron. Astrophys. **641**, A6 (2020).

[16] A. G. Riess, S. Casertano, W. Yuan, L. M. Macri, and D. Scolnic, Astrophys. J. **876**, 85 (2019).

[17] E. Mortsell, A. Goobar, J. Johansson, and S. Dhawan, arXiv:2105.11461.

[18] W. L. Freedman, Astrophys. J. **919**, 16 (2021).

[19] A. Starobinsky, Phys. Lett. B **91**, 99 (1980).

[20] K. Bamba, S. Nojiri, S. O. Odintsov, and D. Sáez-Gómez, Phys. Lett. B **730**, 136 (2014).

[21] G. Tino, L. Cacciapuoti, S. Capozziello, G. Lambiase, and F. Sorrentino, Prog. Part. Nucl. Phys. **112**, 103772 (2020).

[22] V. K. Oikonomou and N. Karagiannakis, Classical Quantum Gravity **32**, 085001 (2015).

[23] T. P. Sotiriou and V. Faraoni, Rev. Mod. Phys. **82**, 451 (2010).

[24] T. Faulkner, M. Tegmark, E. F. Bunn, and Y. Mao, Phys. Rev. D **76**, 063505 (2007).

[25] S. Capozziello and S. Tsujikawa, Phys. Rev. D **77**, 107501 (2008).

[26] J.-Q. Guo, Int. J. Mod. Phys. D **23**, 1450036 (2014).

[27] T. Chiba, T. L. Smith, and A. L. Erickcek, Phys. Rev. D **75**, 124014 (2007).

[28] W. Hu and I. Sawicki, Phys. Rev. D **76**, 064004 (2007).

[29] G. Cognola, E. Elizalde, S. Nojiri, S. D. Odintsov, L. Sebastiani, and S. Zerbini, Phys. Rev. D **77**, 046009 (2008).

[30] S. D. Odintsov, D. Sáez-Chillón Gómez, and G. S. Sharov, Eur. Phys. J. C **77**, 862 (2017).

[31] Y. Chen, C.-Q. Geng, C.-C. Lee, L.-W. Luo, and Z.-H. Zhu, Phys. Rev. D **91**, 044019 (2015).

[32] H. Desmond and P. G. Ferreira, Phys. Rev. D **102**, 104060 (2020).

[33] A. P. Naik, E. Puchwein, A.-C. Davis, and C. Arnold, Mon. Not. R. Astron. Soc. **480**, 5211 (2018).

[34] R. C. Nunes, S. Pan, E. N. Saridakis, and E. M. C. Abreu, J. Cosmol. Astropart. Phys. 01 (2017) 005.

[35] C. R. Farrugia, J. Sultana, and J. Mifsud, Phys. Rev. D **104**, 123503 (2021).

[36] R. D'Agostino and R. C. Nunes, Phys. Rev. D **100**, 044041 (2019).

[37] R. D'Agostino and R. C. Nunes, Phys. Rev. D **101**, 103505 (2020).

[38] S. D. Odintsov, D. Sáez-Chillón Gómez, and G. S. Sharov, Nucl. Phys. **B966**, 115377 (2021).

[39] E. Lusso, G. Risaliti, E. Nardini, G. Bargiacchi, M. Benetti, S. Bisogni, S. Capozziello, F. Civano, L. Eggleston, M. Elvis *et al.*, Astron. Astrophys. **642**, A150 (2020).

[40] X. Li, R. E. Keeley, A. Shafieloo, X. Zheng, S. Cao, M. Biesiada, and Z.-H. Zhu, Mon. Not. R. Astron. Soc. **507**, 919 (2021).

[41] G. Bargiacchi, M. Benetti, S. Capozziello, E. Lusso, G. Risaliti, and M. Signorini, arXiv:2111.02420.

[42] Á. de la Cruz-Dombriz, P. K. S. Dunsby, S. Kandhai, and D. Sáez-Gómez, Phys. Rev. D **93**, 084016 (2016).

[43] A. De Felice and S. Tsujikawa, Living Rev. Relativity **13**, 3 (2010).

[44] P. Brax, C. van de Bruck, A.-C. Davis, and D. J. Shaw, Phys. Rev. D **78**, 104021 (2008).

[45] L. Hui, A. Nicolis, and C. W. Stubbs, Phys. Rev. D **80**, 104002 (2009).

[46] C. Negrelli, L. Kraiselburd, S. J. Landau, and M. Salgado, Phys. Rev. D **101**, 064005 (2020).

[47] A. A. Starobinsky, JETP Lett. **86**, 157 (2007).

[48] E. V. Linder, Phys. Rev. D **80**, 123528 (2009).

[49] J. Simon, L. Verde, and R. Jimenez, Phys. Rev. D **71**, 123001 (2005).

[50] D. Stern, R. Jimenez, L. Verde, M. Kamionkowski, and S. A. Stanford, J. Cosmol. Astropart. Phys. 02 (2010) 008.

[51] M. Moresco, A. Cimatti, R. Jimenez, L. Pozzetti, G. Zamorani, M. Bolzonella, J. Dunlop, F. Lamareille, M. Mignoli, H. Pearce *et al.*, J. Cosmol. Astropart. Phys. 08 (2012) 006.

[52] C. Zhang, H. Zhang, S. Yuan, S. Liu, T.-J. Zhang, and Y.-C. Sun, Res. Astron. Astrophys. **14**, 1221 (2014).

[53] M. Moresco, Mon. Not. R. Astron. Soc. **450**, L16 (2015).

[54] M. Moresco, L. Pozzetti, A. Cimatti, R. Jimenez, C. Maraston, L. Verde, D. Thomas, A. Citro, R. Tojeiro, and D. Wilkinson, J. Cosmol. Astropart. Phys. 05 (2016) 014.

[55] D. M. Scolnic, D. O. Jones, A. Rest, Y. C. Pan, R. Chornock, R. J. Foley, M. E. Huber, R. Kessler, G. Narayan, A. G. Riess *et al.*, Astrophys. J. **859**, 101 (2018).

[56] A. G. Riess, S. Casertano, W. Yuan, L. Macri, J. Anderson, J. W. MacKenty, J. B. Bowers, K. I. Clubb, A. V. Filippenko, D. O. Jones *et al.*, Astrophys. J. **855**, 136 (2018).

[57] C. Negrelli, L. Kraiselburd, S. Landau, and C. G. Scóccola, J. Cosmol. Astropart. Phys. 07 (2020) 015.

[58] J. L. Bernal, T. L. Smith, K. K. Boddy, and M. Kamionkowski, Phys. Rev. D **102**, 123515 (2020).

[59] A. J. Ross, L. Samushia, C. Howlett, W. J. Percival, A. Burden, and M. Manera, Mon. Not. R. Astron. Soc. **449**, 835 (2015).
[60] E. A. Kazin, J. Koda, C. Blake, N. Padmanabhan, S. Brough, M. Colless, C. Contreras, W. Couch, S. Croom, D. J. Croton *et al.*, Mon. Not. R. Astron. Soc. **441**, 3524 (2014).
[61] M. Ata, F. Baumgarten, J. Bautista, F. Beutler, D. Bizyaev, M. R. Blanton, J. A. Blazek, A. S. Bolton, J. Brinkmann, J. R. Brownstein *et al.*, Mon. Not. R. Astron. Soc. **473**, 4773 (2018).
[62] T. M. C. Abbott, F. B. Abdalla, A. Alarcon, S. Allam, F. Andrade-Oliveira, J. Annis, S. Avila, M. Banerji, N. Banik, K. Bechtol *et al.*, Mon. Not. R. Astron. Soc. **483**, 4866 (2019).
[63] S. Alam, M. Ata, S. Bailey, F. Beutler, D. Bizyaev, J. A. Blazek, A. S. Bolton, J. R. Brownstein, A. Burden, C.-H. Chuang *et al.*, Mon. Not. R. Astron. Soc. **470**, 2617 (2017).
[64] J. E. Bautista, R. Paviot, M. Vargas Magaña, S. de la Torre, S. Fromenteau, H. Gil-Marín, A. J. Ross, E. Burtin, K. S. Dawson, J. Hou *et al.*, Mon. Not. R. Astron. Soc. **500**, 736 (2020).
[65] R. Neveux, E. Burtin, A. de Mattia, A. Smith, A. J. Ross, J. Hou, J. Bautista, J. Brinkmann, C.-H. Chuang, K. S. Dawson *et al.*, Mon. Not. R. Astron. Soc. **499**, 210 (2020).
[66] J. E. Bautista, N. G. Busca, J. Guy, J. Rich, M. Blomqvist, H. du Mas des Bourboux, M. M. Pieri, A. Font-Ribera, S. Bailey, T. Delubac *et al.*, Astron. Astrophys. **603**, A12 (2017).
[67] H. du Mas des Bourboux, J.-M. Le Goff, M. Blomqvist, N. G. Busca, J. Guy, J. Rich, C. Yèche, J. E. Bautista, E. Burtin, K. S. Dawson *et al.*, Astron. Astrophys. **608**, A130 (2017).
[68] G. Risaliti and E. Lusso, Astrophys. J. **815**, 33 (2015).
[69] G. Risaliti and E. Lusso, Nat. Astron. **3**, 272 (2019).
[70] G. Bargiacchi (private communication).
[71] N. Khadka and B. Ratra, Mon. Not. R. Astron. Soc. **502**, 6140 (2021).
[72] N. Khadka and B. Ratra, Mon. Not. R. Astron. Soc. **510**, 2753 (2022).
[73] O. Luongo, M. Muccino, E. Ó. Colgáin, M. M. Sheikh-Jabbari, and L. Yin, arXiv:2108.13228.
[74] P. Virtanen, R. Gommers, T. E. Oliphant, M. Haberland, T. Reddy, D. Cournapeau, E. Burovski, P. Peterson, W. Weckesser, J. Bright *et al.*, Nat. Methods **17**, 261 (2020).
[75] D. Foreman-Mackey, D. W. Hogg, D. Lang, and J. Goodman, Publ. Astron. Soc. Pac. **125**, 306 (2013).
[76] M. Leizerovich, fR-MCMC, https://github.com/matiasleize/fR-MCMC (2021).
[77] K. C. Wong, S. H. Suyu, G. C.-F. Chen, C. E. Rusu, M. Millon, D. Sluse, V. Bonvin, C. D. Fassnacht, S. Taubenberger, M. W. Auger *et al.*, Mon. Not. R. Astron. Soc. **498**, 1420 (2020).
[78] S. Basilakos, S. Nesseris, and L. Perivolaropoulos, Phys. Rev. D **87**, 123529 (2013).
[79] R. C. Nunes (private communication).